ISSN 1392 – 124X INFORMATION TECHNOLOGY AND CONTROL, 2011, Vol.40, No.1

LATTICE PWL MODELING OF SEPARABLE CONVEX FUNCTIONS AND ITS APPLICATION TO THE VEHICLE FOLLOWING PROBLEM

Junaid M. Khan*, Shuning Wang

National University of Sciences and Technology
Islamabad, Pakistan
e-mail: contactjunaid@yahoo.com, swang@mails.tsinghua.edu.cn

crossref http://dx.doi.org/10.5755/j01.itc.40.1.193

Abstract. Due to the inherent nonlinear nature of real world systems, one of the most popular ways to deal with nonlinear systems is to find a feedback linearizing input and then deal with the system by using the rich literature on linear control methods. As an alternative, the nonlinear terms in the system model can be piecewise linearized and then the system can be controlled by using various linear control approaches. The purpose of this paper is to show that under certain conditions, piecewise linearization (PWL) outperforms feedback linearization. In this note, a systematic procedure is outlined for approximating convex separable nonlinear systems with a continuous piecewise linear function and, to emphasize upon the basic idea of this paper, a widely employed nonlinear vehicle following model is used as an example. For this particular model, it is shown that the approximation scheme is optimal with respect to the number of local linear models and the inherent problem of increased dimensionality of PWL systems is not significant. As an extension of our previous work, it is also shown that parametric uncertainties can be deeply investigated, which is not possible in the case of feedback linearization. A simulation study is carried out to show that the proposed system not only guarantees asymptotic tracking of the desired trajectories, but also ensures safety and ride comfort under the constraints of physical limitations inherent in the system. Various issues of vehicle following, e.g. convergence of error in the inter-vehicle spacing, velocity following, control saturation and parametric uncertainties are addressed in this paper. The performance analysis reveals that this new strategy yields promising results.

Keywords: nonlinear system approximation, piecewise linear function, automatic cruise control.

1. Introduction

Approximation and control of nonlinear functions by Piecewise linear (PWL) functions has undergone a wealth of theoretical development as evidenced by growing list of research articles dedicated to the subject e.g. [1-20], etc. The reasons suggesting it worthwhile to investigate PWL systems are that PWL systems are simple to implement and offer ease of theoretical analysis and calculation. Despite a significant surge of interest in representation of PWL systems, the recent research has seen limited practical implementations. Some detailed applications are found in the field of nonlinear circuits analysis e.g. [3, 7, 11] whereas many researches contain brief applications and the main focus of such researches was to validate their proposed PWL algorithms as in [2, 8, 13, 18, 19]. Nevertheless there exist research articles e.g. [15, 16, 17] which deal with specific systems for their respective control issues. The reason, why PWL models are not widely applied, lies in that the conventional representations of PWL functions are concerned with too many parameters which occur in the functions expression and the domain partitions. The complexity of PWL modeling and control depends upon the number of nonlinearities, type of nonlinearities, domain of the variables representing the nonlinear function and the required precision of approximation to the original nonlinear model.

As performance demands on modern control systems increase, controllers are required to work over large operating ranges where assumptions on linear dynamics are no longer valid. To control a nonlinear system around a specific operating point, a set of linear models in a local region has been widely used. For such a system, the controller parameters are changed to the appropriate values corresponding to the equilibrium points. But this approach generally requires a large number of controllers, otherwise the operating range is too limited. More number of controllers entails frequent switching of controllers which may lead to instability. On the other hand, by using piecewise linear local models the state space region can be investigated incrementally.

Feedback linearization is another commonly adopted approach to deal with the nonlinear systems [21,

22, 24-28, 30]. It may be noted that feedback linearization of the system requires exact measurement of system parameters, which is sometimes hard to determine precisely, especially in case of parametric variations. Though useful sometimes, however in many cases an unwanted result of feedback linearization is the modification of the system, thus loosing details by neglecting important dynamics and simplification of the original model to an undesired extent. So there exists a need to deal with the system model in its (as far as possible) original form.

In this paper we adopt a continuous PWL model to approximate the nonlinear vehicle following model (VFM) and hence present a stable piecewise linear control approach. The contributions and novelty of this work can be mainly attributed to the PWL approximation and control of a widely employed nonlinear vehicle following model. The resulting PWL model is simple, represents the entire domain of interest, valid over a wider region, and hence we show that a fewer number of linear models are enough to approximate the complete system.

The research on VFM sees a number of articles where the authors have used the same nonlinear model (as in this paper) and then applied their linear control approaches to demonstrate the effectiveness of their vehicle following algorithms. In fact, there exist two basic trends in using the specific VFM: one is to use its most simple linearized form at the first instance [31-36] and then use different linear controls for vehicle tracking; the other trend is to use the model in original nonlinear form at the first instance, then perform feedback linearization and then use some preferred linear control method e.g. PID, state feedback, Linear Quadratic Control (LQR) or H-infinity.

Both of these approaches have been successful in offering useful results, nevertheless each of these bears some fundamental problems. The model used according to the first trend is too simple and just represents the movement of two masses and doesn't account for many important factors which affect the dynamics of vehicles, while the second trend actually follows the first one in spirit, as it is based on finding a feedback linearizing control which cancels the nonlinear terms and transforms the model in the same form as is used under the first trend. With either of these trends, the resulting model and the consequent control results suffer from major disadvantages such as: if the feedback linearization is successful, the control disregards the effects of nonlinear term and certain factors (will be covered in detail in Sections 3 and 5); any disturbance in the parameters would render the linearization process inexact and hence the control would not be effective. Our adopted approach differs from both of these trends and is able to account for these fundamental disadvantages.

The approach adopted in this work splits the system into the constituent linear continuous subsystems, and the boundaries of subsystems are determined in a methodical way. As an extension of our previous work [20], we show that the modeling scheme is optimal with respect to the number of local models and is the best approximation for the original model. We apply this modeling approach on the nonlinear VFM (used in [21-30]) and then design linear control valid for each local linear model. The switching logic of controllers is based on the current value of the measured state, hence a self-organizing scheme is developed where the controllers switch according to present value of the measured signal. We perform the control of a follower vehicle which keeps a fixed or variable-over-speed distance with a leader vehicle. Then we address various aspects of regulation and tracking of the desired distance and velocity under the constraints and limitations inherent in the actual plant. The applicability of the proposed method is demonstrated by simulations, where the robustness properties of the control system are also evaluated against parametric uncertainties.

The remainder of the paper is organized as follows: In Section 2, the PWL modeling scheme is described. In Section 3, the scheme is applied to approximate a third order nonlinear vehicle following model. Section 4 discusses controller design and implementation. In Section 5, the performance of the system is evaluated by simulations. The simulations include possible real state scenarios and different maneuvers. Finally conclusions are drawn in Section 6.

2. System Representation by PWL Functions

The first PWL absolute value model was proposed by Kang and Chua [14] which can represent all one-dimensional (1-D) continuous PWL functions, and also a part of the 2-D continuous PWL functions that possess the consistent variation property. Thereafter, Kahlert and Chua improved the model to represent all 2-D continuous PWL functions [4]. A more general model proposed by Lin can theoretically represent all continuous PWL functions [5]. On the whole, the existing global representation of PWL functions is limited to the continuous PWL functions, the forms of which include the absolute value form, minimum-maximum form and state equation form. The canonical PWL representation, which was first introduced in [14] for analyzing nonlinear circuits, has been a successful example. It is a linear combination of a linear (affine) function and a number of absolute-value functions of linear functions. Its scalar form can be written as:

$$l(x \mid \theta(0)) + \sum_{i=1}^{m} c_i \left| l(x \mid \theta(i)) \right|, \qquad (1)$$

where $l(\cdot \mid \theta(i)): R^n \to R$ denotes a linear function determined by a parameter vector $\theta(i) \in R^{n+1}$, i.e., $l(x \mid \theta(i)) = \begin{bmatrix} 1 & x^T \end{bmatrix} \theta(i)$, $\forall x \in R^n$. On the other

hand, there exists a totally different way to represent a continuous PWL function. It is called a lattice PWL function [9]. The general form of this representation for PWL functions that consist of *m* local linear functions is:

$$\min_{1\le i\le M}\ \max_{j\in s_i} l(x\,|\,\theta(j)). \qquad (2)$$

Each s_i is a nonempty subset of the index set Z_m={1,2,…m}, M is a positive integer [11] denoting the total number of subsets s (M>m) and m is the total number of local linear functions which are used to approximate the nonlinear function. As equation (2) must equal one of $l(x\,|\,\theta(1))$, $l(x\,|\,\theta(2))$, …., $l(x\,|\,\theta(m))$ for any $x\in R^n$, it is indeed a continuous PWL function whose local linear functions are just $l(x\,|\,\theta(j))$. In order to find a general representation that consists of at most *n*-level nestings of absolute-value functions for all continuous PWL functions in *n* dimensions, it is sufficient to find such a representation for the convex function:

$$\max_{j\in Z_m} l(x\,|\,\theta(j)). \qquad (3)$$

Now consider a nonlinear dynamic system:

$$\begin{aligned}\dot{\mathrm{x}}(t) &= \mathrm{G}(\mathrm{x}(t),\mathrm{u}(t)),\\ \mathrm{y}(t) &= \mathrm{C}(\mathrm{x}(t))\end{aligned} \qquad (4)$$

where G is the nonlinear function, x is the state vector ($\mathrm{x}\in R^n$), $\mathrm{y}\in R^p$ is the measured output, and $\mathrm{u}\in R^q$ is the input. More explicitly, $\{G_1, G_2, G_3, ...G_n\}$ are the nonlinear functions for the respective 1st order state equations as given below:

$$\begin{aligned}\dot{x}_1(t) &= G_1\{x_1(t), x_2(t), ...x_n(t), u_1, u_2, ...u_q\}\\ \dot{x}_2(t) &= G_2\{x_1(t), x_2(t), ...x_n(t), u_1, u_2, ...u_q\}\\ &\vdots \qquad\qquad \vdots\\ \dot{x}_n(t) &= G_n\{x_1(t), x_2(t), ...x_n(t), u_1, u_2, ...u_q\}\end{aligned}$$

Let each component of G i.e. $\{G_1, G_2, G_3, ...G_n\}$ be a separable function which is a sum of (n+q) univariate functions i.e. $G_k(x) = \sum_{j=1}^{n}\overline{G}_{k,j}(x_j) + \sum_{j=1}^{q}\overline{G}_{k,j}(u_j)$ for any $k = 1, 2, ...n$ where $\overline{G}_{k,j}$ is a univariate nonlinear function. Since every G_k is the sum of $n+q$ univariate functions $\overline{G}_{k,j}$ $(1\le j\le n+q)$, so approximating each $\overline{G}_{k,j}$ by a univariate CPWL function will result in the CPWL approximation of G. This can be accomplished by partitioning the region of interest of each univariate function into many non-overlapping small intervals. Let for a pair of indices $\overline{k,j}$, $\overline{G}_{\overline{k,j}}$ be an arbitrary nonlinear convex univariate function whose region of interest is $[a,b]\subset R$. To approximate $\overline{G}_{\overline{k,j}}$ to a satisfactory precision by the linear functions $l(x\,|\,\theta_i) = \beta_i x + \gamma_i$, where $\varsigma_0 = a$, $\varsigma_m = b$, the domain $[a,b]$ has to be divided into $(m-1)$ breakpoints $(a<\varsigma_1<\varsigma_2<.....<\varsigma_{m-1}<b)$. The parameters of each linear segment, i.e. (β_i,γ_i), can be determined by using the scheme outlined in Section 3. Suppose the nonlinear function $\overline{G}_{\overline{k,j}}$ is approximated by a finite number of linear segments. A CPWL approximation function $P(x)$ of $\overline{G}_{\overline{k,j}}$ on [*a, b*] can be obtained by connecting these linear segments as follows:

$$\overline{G}_{\overline{k,j}}(x) \simeq P(x) = \max\{l_1(x), l_2(x), l_3(x), ...l_m(x)\}, \qquad (5)$$

where $l_1(x), l_2(x), ...l_m(x)$ are local linear functions approximating the nonlinear function. Our goal is to use the least number of linear segments out of $l_1(x), l_2(x), ...l_m(x)$ such that the following function is minimized over a finite interval ($a\to b$):

$$\min\left\{\max_{x\in[a,b]}\left|\overline{G}_{\overline{k,j}}(x) - P(x)\right|\right\}. \qquad (6)$$

The scheme so far explained can be generally applied to the systems containing many convex univariate nonlinearities, however from here onwards we restrict our discussion to the VFM, which contains only one quadratic nonlinearity.

3. Vehicle following model

A configuration of leader-follower is given by the choice of the following variables as listed below:

x_l – Distance of the leader from a reference point

x_f – Distance of the follower from a reference point

L – Length of the vehicle

v_f – Velocity of the follower

f_f – Propulsion force

m_f – Mass of the vehicle

x_e – Error in the desired distance to be maintained

δ – Intervehicle spacing between two vehicles

v_l – Velocity of the leader

T_f – Engine time constant of the vehicle

K_{ad} – Aerodynamic drag coefficient of the vehicle

K_{md} – A constant mechanical drag on the vehicle

$d_{1f}(t)$ – Disturbance input

From Newton's Second Law, the relationship between the acceleration of the follower vehicle, its propulsion force and the drag forces acting on it can be derived as:

$$m_f\ddot{x}_f = f_f - K_{ad}\dot{x}_f^{\,2} - K_{md} + d_{1f}(t). \qquad (7)$$

The propulsion system which represents the engine dynamics of the vehicle can be modeled as a first order system:

$$\dot{f}_f = \frac{1}{T_f}(-f_f + u)\,. \tag{8}$$

This model requires the following simplifying assumptions. (i) The motion of the vehicles is constrained to translations only (ii) The movement of vehicles is smooth. (iii) The follower is equipped with sensors to measure the relative distance between the two vehicles, its velocity and acceleration. Let $\delta = x_f - x_l - L$, then with the choice of state vector $x = \begin{bmatrix} \delta & v_f & f_f \end{bmatrix}^T$, where $v_f = \dot{x}_f$, we can transform equations (7) and (8) as below:

$$\begin{aligned} \dot{\delta} &= v_l - v_f \\ \dot{v}_f &= \frac{1}{m_f}\left[(f_f - K_{d_f} v_f^{\,2} - K_{md} + d_{1_f}(t)\right]. \\ \dot{f}_f &= \frac{1}{T_f}(-f_f + u) \end{aligned} \tag{9}$$

3.1. PWL Modeling for VFM

The state equations given by (9) form a convex separable nonlinear function which contains one nonlinearity, i.e. $\overline{G_{k,j}} = v_f^2$. The domain of interest for follower velocity is chosen as [0, 20], i.e. [0 km/hr, 72 km/hr]. The goal is to find a piecewise linear function $P(x)$, which can approximate the nonlinear function. According to equation (3), the following procedure can be adopted and a number of linear functions can be computed to achieve an arbitrary precision to the original function $\overline{G_{k,j}}$ as shown in Figure 1.

(i) Find the linear approximation $L_1(x)$ over the entire domain/interval of interest.

(ii) Find $\varsigma_1 = \arg\limits_x \left[\max \left\{ L_1(x) - \overline{G_{k,j}} \right\} \right]$.

(iii) Find the linear function $l_1(x)$ for the first partition which originates from $\overline{G_{k,j}}(0)$ and intersects $\overline{G_{k,j}}(x)$ at ς_1.

(iv) From this point on $\overline{G_{k,j}}(\varsigma_1)$, draw another linear approximation $L_2(x)$ for the remaining interval.

(v) Find $\varsigma_2 = \arg\limits_x \left[\max \left\{ L_2(x) - \overline{G_{k,j}}(x) \right\} \right]$.

(vi) Find the second linear function $l_2(x)$ passing through $\overline{G_{k,j}}(\varsigma_1)$ and intersecting $\overline{G_{k,j}}(x)$ at ς_2 ...and so on.

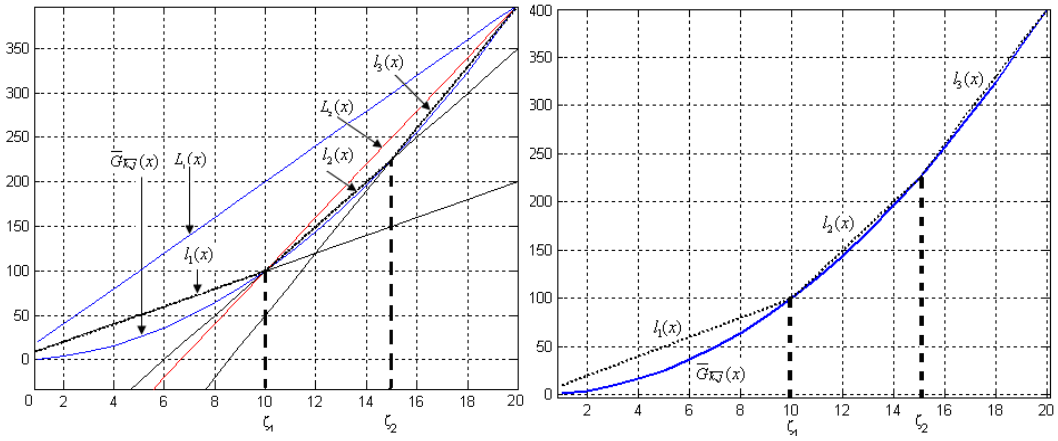

Figure 1. A convex function $\overline{G_{k,j}}(x)$ approximated by a PWL function containing 3 linear functions

The procedure stated above can be continued and a number of linear functions can be computed until an arbitrary precision to the original nonlinear function is achieved. The scheme mentioned in (i) through (vi) will sequentially partition the whole state space into constituent non-overlapping linear regions. For the case shown in Figure 1, $\overline{G_{k,j}}(x)$ is approximated by $P(x)$ as follows:

$$\overline{G_{k,j}}(x) \simeq P(x) = \max\left\{l_1(x), l_2(x), l_3(x)\right\} \tag{10}$$

In the state space form, the system can be expressed as:

$$\begin{aligned} \dot{x}(t) &= A_i(\theta_i)x + B_i u_i(t)\,, \\ y(t) &= C_i(x(t)) \end{aligned} \tag{11}$$

where A_i and C_i are real matrices of compatible dimensions and $y(t) = \delta$ i.e. error in the desired spacing between two vehicles. We refer to θ_i as the mode in force at time *i*, thus every operating region will induce a corresponding mode, which means that for every approximating linear function, there will be a corresponding matrix *A*. This is different from the switched linear systems [15] [38], in which the mode θ_i is an exogenous variable that is completely independent of the state history.

3.2. Optimality of PWL Approximation for VFM

The choice of a suitable number of linear functions can be based on the physical performance of the system and can be set according to the following algorithm.

(a) Choose an arbitrary *m* and partition the region of interest according to the method explained in subsection 3.1.

(b) Apply the control scheme and obtain the error defined as $\varepsilon(x) = \|y_d - y\|$, where y_d is the desired output.

(c) If the error measure is sufficiently large such that the performance of the system is not acceptable, increase the number of partitions to $m+1$, apply the control, observe $\varepsilon(x)$ and related performance.

(d) Repeat (c) unless a suitable performance is achieved.

(e) For an arbitrarily chosen *m*, if the error implies a suitable performance, reduce the partitions to *m*-1, observe $\varepsilon(x)$ and related performance.

(f) Repeat (e) unless a suitable performance is continued to be achieved. The least number of partitions, or equivalently, number of local linear functions thus obtained would be the optimal one.

Since in the case of approximating nonlinear term of VFM (i.e. $v_f^{\,2}$ of equation (9)), the domain of interest of the nonlinear term can be reasonably taken as [0,20] m/sec. Then by using the method of subsection 3.1, it is seen that the first linear segment will coincide with the nonlinear function at half way i.e. $\varsigma_1 = 10$ as illustrated in Figure 1. Hence it is not difficult to see graphically that if only two segments are used for approximating this nonlinear convex function, then the partition at $\overline{G_{k,j}}(\varsigma_1)$, will allow having the best fit for $\overline{G_{k,j}}(x)$. This fact can be explained with the following derivation as given next. It is required that:

$$D = \left[\left|\left\{\int_0^{\varsigma_1} l_1(x)dx + \int_{\varsigma_1}^{20} L_2(x)dx\right\} - \int_0^{20} \overline{G_{k,j}}(x)dx\right|\right]$$

is minimum. (12)

In the following, we prove the statement of equation (12) by computing the value of an arbitrary ς_1 and hence show that the modeling scheme is optimal. The area between the curve $\overline{G_{k,j}}$ and its linear approximation, as shown in Figure 1, is given by $\int_0^{20}\int_0^{x^2} d\overline{G_{k,j}}dx = C$. Now for the case when the nonlinear function $\overline{G_{k,j}}$ is approximated by two linear segments partitioned at point ς_1, the area will be given by:

$$D(\varsigma_1) = \int_{x=0}^{x=\varsigma_1}\int_{\overline{G_{k,j}}=0}^{\overline{G_{k,j}}=\varsigma_1 x} d\overline{G_{k,j}}dx + \int_{x=\varsigma_1}^{x=20}\int_{\overline{G_{k,j}}=0}^{\overline{G_{k,j}}=x(20+\varsigma_1)-20\varsigma_1} d\overline{G_{k,j}}dx - C,$$

$$D(\varsigma_1) = \int_{x=0}^{x=\varsigma_1} \varsigma_1 x dx + \int_{x=\varsigma_1}^{x=20} \{x(20+\varsigma_1) - 20\varsigma_1\}dx - C,$$

$$D(\varsigma_1) = \frac{\varsigma_1^{\,3}}{2} + 4000 - 200\varsigma_1 + 10\varsigma_1^{\,2} - \frac{\varsigma_1^{\,3}}{2} - C,$$

$$D(\varsigma_1) = 10\varsigma_1^{\,2} - 200\varsigma_1 + 4000 - C. \quad (13)$$

Equation (13) depicts the area between $\overline{G_{k,j}}$ and the two linear segments meeting at ς_1. To optimize (13), we find the minimum value of $D(\varsigma_1)$ by letting $\frac{\partial D(\varsigma_1)}{\partial \varsigma_1} = 0$, $\Rightarrow 20\varsigma_1 - 200 = 0$, $\Rightarrow \varsigma_1 = 10$ which is the mid value, therefore the requirement in (12) is satisfied. Similarly the fact that $\left[\left|\int_{\varsigma_1}^{20} \overline{G_{k,j}}(x)dx - \left\{\int_{\varsigma_1}^{\varsigma_2} l_2(x)dx + \int_{\varsigma_2}^{20} l_3(x)dx\right\}\right|\right]$ is minimum and the point ς_2 can be derived as in the former case.

It can be observed that when the method of subsection 3.1 is adopted and as we move away from the origin, the approximation gets finer and closer to the original function. This feature facilitates the considered VFM in a natural way. As in the original model, the nonlinearity exists on the velocity variable. Therefore as the velocity increases, the approximation accuracy also improves. This is fortunate, because in case of higher velocity the safety factor requires that the control action be implemented with higher precision. However this situation is only suitable where a constant headway is maintained between the vehicles. For a speed-dependent spacing policy, however, slow moving vehicles will require lesser spacing, which in turn requires more precision from the safety viewpoint. In such a case, the first partition could be performed as:

$$\varsigma_1 = \frac{1}{2}\arg\left[\max_x \left\{L_1(x) - \overline{G_{k,j}}(x)\right\}\right]. \quad (14)$$

It is worth noting that in the abundant literature (referenced in Section 2), using the same VFM and employing feedback linearization, the resulting model is simplified to an extent such that the control disregards the effects of forces such as aerodynamic drag, mechanical drag and any other disturbances, hence instead of designing a controller to take such factors into account, the system dynamics are simplified to

suit the controller, whereas our work becomes more promising in the sense that that the PWL model retains all such omitted factors.

4. Control Design

The control objective is to design *u(t)* in such a way that inter-vehicle spacing tracks a desired reference, where *u(t)* can be viewed as the throttle/brake input causing acceleration/decelerations in the controlled vehicle. Since the adopted approach involves decomposition of the original system to many non-overlapping linear systems, it is desired to have the same number of linear controllers where each is valid for the corresponding linear system, i.e.

$$\begin{aligned} &u_1(t) \to A_1(\theta_1(t)) \\ &u_2(t) \to A_2(\theta_2(t)) \\ &\quad\cdot \qquad\cdot \qquad . \\ &\quad\cdot \qquad\cdot \\ &u_m(t) \to A_m(\theta_m(t)) \end{aligned}$$

Using the computed parameters (β_i, γ_i) of local linear models, the matrices A_i $(i = 1,2,..m)$ are determined. The controllability matrices for each local model are tested for full rank condition and once a positive result for each matrix is obtained, it is concluded that each $\left[A_i \;\; B_i\right], (i = 1,2,..m)$ pair is controllable. Therefore a state feedback control can be designed to achieve stability by placing the eigen-values of each system in the negative half of the imaginary axis. The theoretical proofs for controllability analysis and stability of PWL systems using a state feedback control are stated in detail in [6]. In this work the computation of state feedback control vector is based on the linear quadratic control method where:

$$\begin{aligned} &u_1(t) = -k_1 x(t) \\ &u_2(t) = -k_2 x(t) \\ &\quad\cdot \qquad\cdot \qquad . \\ &\quad\cdot \qquad\cdot \\ &u_m(t) = -k_m x(t) \end{aligned} \qquad (15)$$

Each k_i is an *n*-dimensional real row vector which is obtained for the closed loop system such that the performance index $J = \int_0^\infty \{\mathrm{x}^*(t) Q \mathrm{x}(t) + u_i^2(t)\} dt$ is minimized, where Q is a positive semidefinite Hermitian or real symmetric matrix. The control vector k_i is obtained as follows: first, the reduced matrix Riccati equation is solved for matrix F_i, and then k_i is computed as below:

$$\begin{aligned} &A_i^T F_i + F_i A_i - F_i B_i B_i^T F_i + Q = 0 \\ &k_i = B_i^T F_i, \; i = \{1,2,...m\} \end{aligned} \qquad (16)$$

The algorithm given in Section 3.2 is applied to the VFM and it is observed that 3 linear functions are enough to approximate the nonlinear function for a satisfactory control performance. The control performance is demonstrated by simulations in Section 5.

4.1. Stability

It can be intuitively seen from the order of VFM given by equation (9) that after designing control for each local linear model, the control vector k_i will have 3 elements in which the second element will differ due to the respective linear model, whereas 1st and 3rd elements will remain unchanged. Substitution of (15) into the dynamic equation (11) will result in formation of closed loop affine continuous PWL system matrices $A_i - B_i k_i$, and the state feedback control u_i will force the eigenvalues of each local $(A_i - B_i k_i)$ matrix to lie in the negative half of the complex plane, therefore according to Theorem 2.4 of [6], the stability of the entire PWL system in the finite domain will be assured.

4.2. Control Implementation

The control scheme is implemented in the SIMULINK environment as shown in Figure 2, where the value of the measured velocity is set as the switching function for scheduling of controllers. In Figure 2 the block named Nonlinear Plant is constructed according to equation (9). The instantaneous value of velocity obtained from the Plant model is fed to a Logic Block, where the switching logic is set on the basis of breakpoints $\varsigma_1, \varsigma_2, ...\varsigma_m$, the value of measured velocity activates only one Action Block, through which the already computed control based on LQR synthesis is relayed to the feedback path.

5. Simulations and Performance Analysis

In the simulation analysis, the parameters as listed in the vehicle modeling section, are assumed as $m_f = 1300$, $T_f = 0.2$, $K_{ad} = 0.3$, $K_{md} = 0.35$. The disturbance profile $d_{1_f}(t)$ (as shown in Figure 3) is a smooth function of time. This disturbance profile is chosen exactly the same as used in [37].

5.1. Regulation of Error in the Desired Spacing

The scenario assumed here is such that the initial error in the desired spacing is 5m, 10m, 15m, 20m, 25m, and 30m, respectively (Figure 4). As the autonomous operation begins, the controllers cause the follower to accelerate/decelerate in order to bring the spacing error to zero, as shown in Figure 4. In doing so, the controllers are supposed to cause acceleration realizable by the physical system, as shown in Figure 5. Physically the response of the controller amounts to acceleration/deceleration (throttle or braking action) of the vehicle, however only in simulations it can be set as high as desired, but practically it has to be set as such to cause realizable acceleration/deceleration. The

maximum applied acceleration/deceleration limits are different for different operating conditions. It has been reported in [26] that ordinary cars can achieve a maximum braking deceleration of $5m/s^2$ and acceleration of $2m/s^2$. Most of the research works in automated driving deal with this constraint by placing a rate limiter in the model. However this approach causes delay in controlled response. In our work, the controller is tuned in such a way that when the leader car accelerates and hence creates a spacing error, the controlled acceleration response of the follower never exceeds the value of applied acceleration of the leader, hence no limiter is needed.

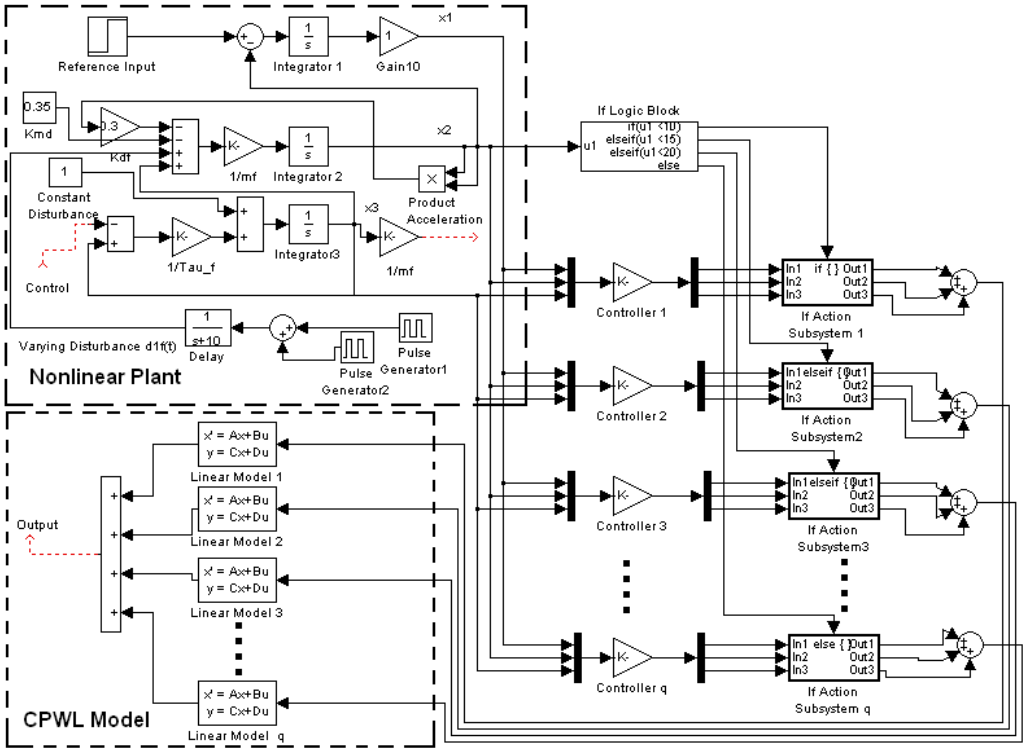

Figure 2. SIMULINK implementation of the PWL modeling and control algorithm

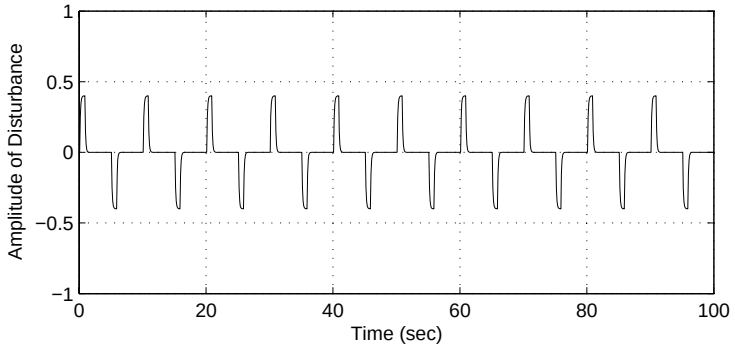

Figure 3. Disturbance input to the vehicle following model

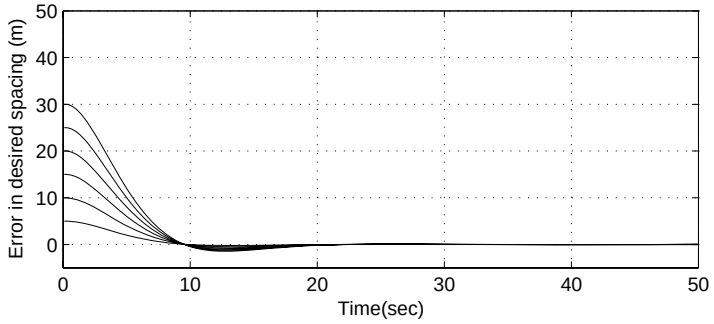

Figure 4. The controlled response of the follower for regulation of errors in the desired distance

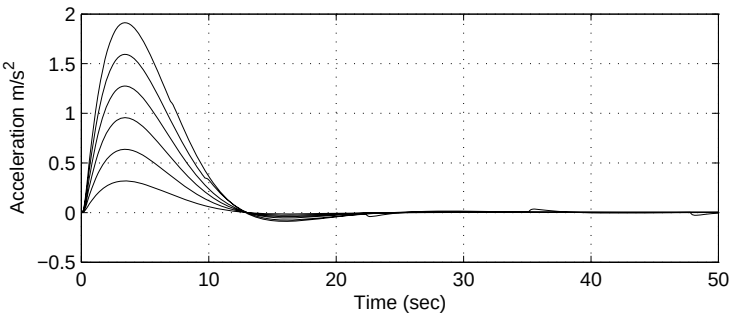

Figure 5. Acceleration response of the follower for regulation of errors in the desired distance

5.2. Velocity Following Case

Resorting to the worst case, the assumed scenario is the leader's hard acceleration/braking maneuver with full throttle (2 m/s^2) and hard brakes (-5 m/s^2). Referring to Figure 6, the initial velocity of both vehicles is the same, however later; leader accelerates for 5 seconds and gets steady at 10 m/sec. Later at 30th instant, the leader again accelerates for 5 seconds with full throttle and then the velocity gets steady at 20 m/sec ($\cong 72 Km/hr$) . At 55th second, it decelerates by applying hard brakes for 5 seconds and finally gets steady at the speed of 5 m/s. The complete maneuver of the leader and controlled follow up of the follower is illustrated in Figure 6. The follower tracks the velocity of leader which is changing rapidly as a result of leader's hard maneuvers. In doing so, the acceleration profile of follower (also given in Figure 6), shows that it catches up with the leader velocity without crossing the available acceleration limits, hence rules out the requirement of any rate limiter. Each of the hard maneuvers is handled by the controlled car in 12 seconds which seems a reasonable settling time from practical point of view.

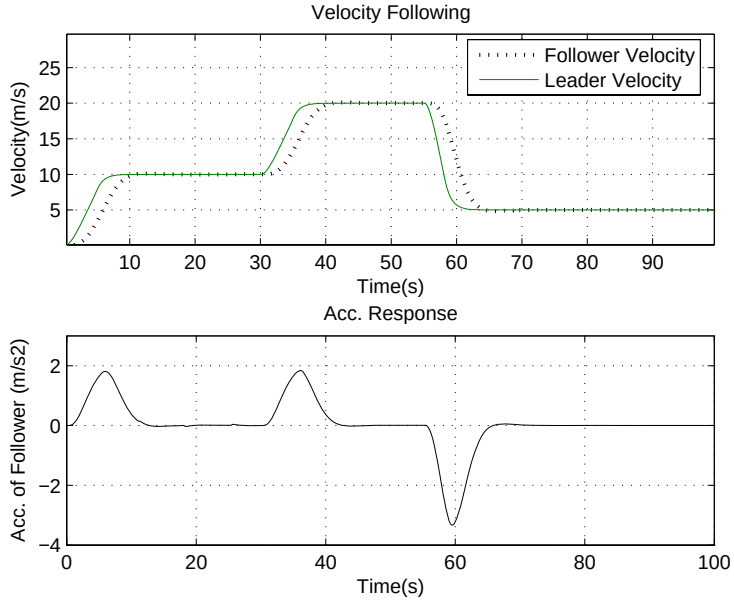

Figure 6. Velocities' profiles of the two vehicles and acceleration response of the follower

5.3. Robustness to Parametric Uncertainties

Realistic vehicle following designs must also address parametric uncertainties such as variations in mass of the vehicle, aerodynamic drag, mechanical drag and engine time constant. The mass of the vehicle varies with the number of passengers and it also varies with the type of vehicle. At small inter-vehicular separations, aerodynamic drag force changes significantly with the distance to be maintained. Because of different types of transmissions, engines and due to usual wear in the machinery, the mechanical drag coefficient and engine time constant vary. With the modeling and control setup mentioned in Sections 3 and 4, the designed system is tested for robustness property against these factors. The nominal mass of vehicle is assumed as 1400 Kg and is then varied to cater for the presence or absence of 4 passengers. The tracking results are shown in Figure 7. From [23], it is learnt that the variations in the mechanical drag coefficient are from 5 to 20 N, the value of K_{md} is varied in simulations for the same controllers' settings. It is observed that the effect of variations of K_{md} is negligibly small as compared to other disturbance terms. For such a case, the response

of the control system is shown in Figure 8. Also from [23] [29], it is known that the aerodynamic drag coefficient varies between 0.05 to 0.5 Kg m^{-1}. The simulation results for varying coefficient are shown in Figure 9. From [28] [29] and [33], the value of T_f lies in the range of 0.25 and 0.8. The control results for such settings are shown in Figure 10. In each of these figures, a zoomed section of the plot is also given which shows that responses for different values of parameters are quite close and thus acceptable.

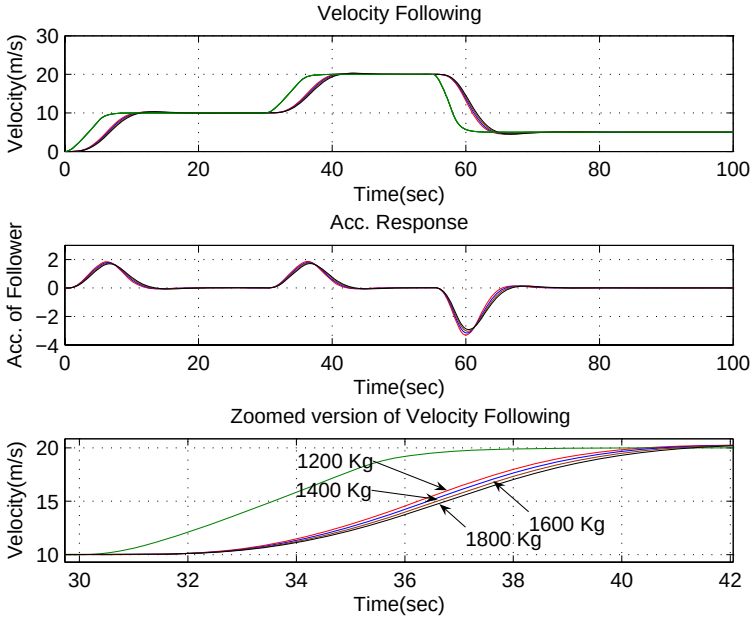

Figure 7. Tracking response for vehicles of different masses, 1200Kg (red) 1400 Kg (blue), 1600 Kg (brown), 1800 Kg (black)

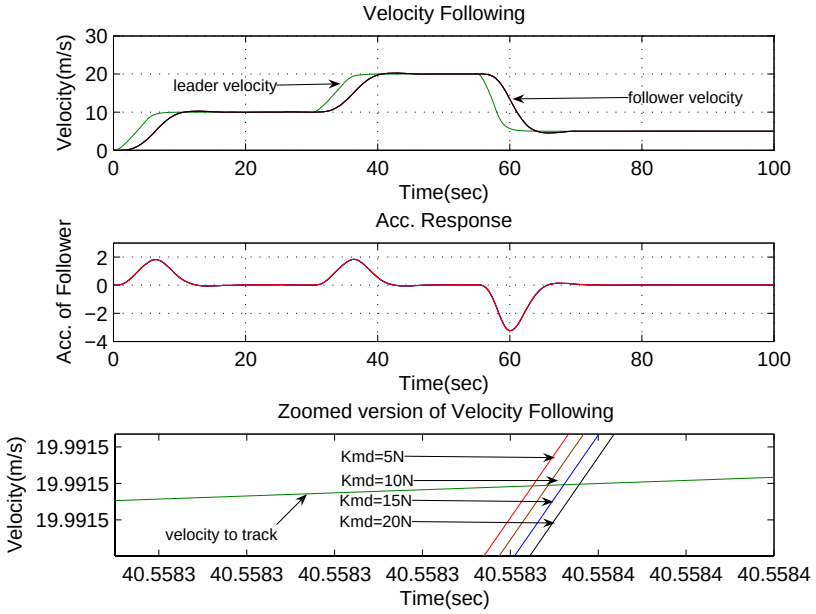

Figure 8. Tracking response for mechanical drag coefficient of 5 N (red), 10 N (brown), 15N (blue) and 20 N (black)

5.4. Safety and Ride Comfort

The issues of safety and ride comfort are the essential elements of an effective vehicle following system, as these factors amount to the nature of controlled response during a follow-up maneuver. Simply safety can be defined in terms of the overshoot and damping of the response, i.e. if the follower vehicle overshoots larger, then it can potentially result in a collision scenario, or if the damping is not suitable, the response will be either having a large overshoot or it will be too delayed. An initiation of another maneuver by leader in the duration of an early follow up would lead to a safety hazard. Ride comfort requires that the frequency and amplitude of controlled response oscillations have to be brought to the minimum. Hence in this work the controller parameters have been carefully tuned to meet these two conditions, as can be seen from the simulation study. However for safety reasons, it is advisable that with

such controller settings, the leader's maneuvers have to be separated by 15 seconds. The small ripples, as seen in the steady state response in Figure 5, are the due to inclusion of the disturbance input.

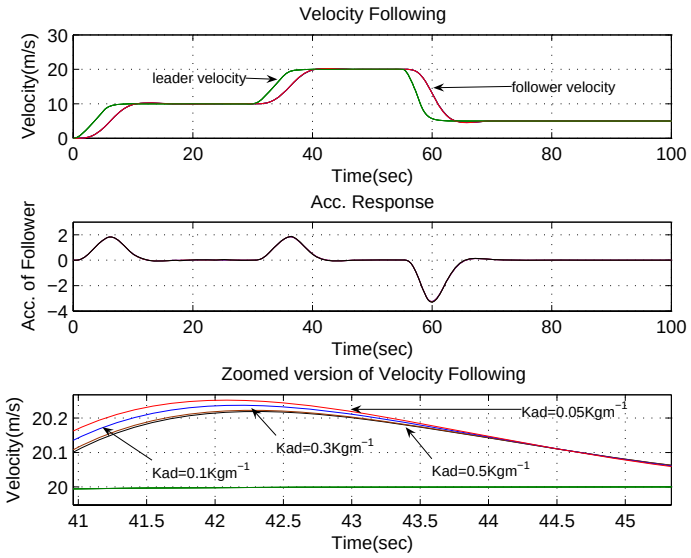

Figure 9. Response for aerodynamic drag coefficient of 0.05 Kgm^{-1}(red), 0.1 Kgm^{-1}(blue), 0.3 Kgm^{-1}(brown) and 0.5 Kg m^{-1}(black)

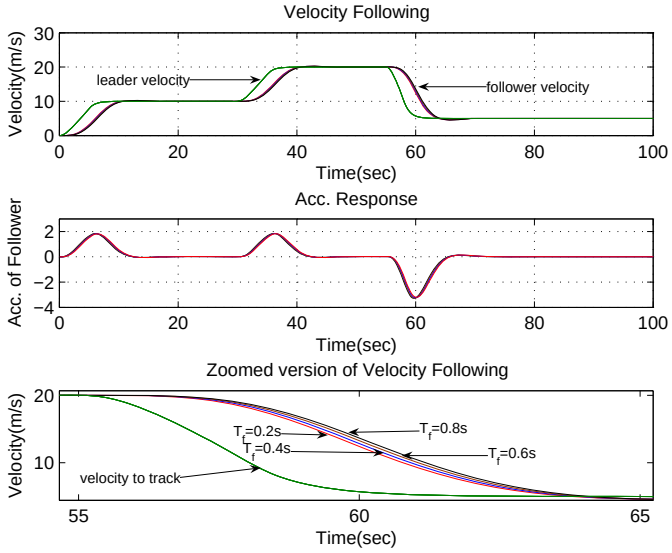

Figure 10. Tracking response for engine time constants of 0.2s (red), 0.4s (blue), 0.6s (brown) and 0.8s (black)

5.5. Comparison to other car following approaches

As already discussed in Section 2, our method relies on approximating rather than nullifying the non-linearity and disturbance factors (aerodynamic drag, mechanical drag etc.), so our method can justifiably outperform other approaches. Also, since according to PWL approximation method, the disturbance terms are not cancelled out, we are able to evaluate the effects of these elements and ascertain the robustness of the control system. Our results, although based on an approximated system, offer the tracking performance evaluated for a number of situations, which is equally good as given by the state of the art work in this area. In Table 1, the control of the PWL model is compared to referenced work in terms of certain factors of performance, e.g. tracking delay, percentage overshoot, settling time etc, however it may be noted that our simulation work contains hard maneuvers, whereas in many of the referenced work, the performance is only evaluated over relaxed maneuvers i.e. accelerations of ≤ 1 m/s^2 To justify the betterment of our approach, the following is worth to mention: the works in [33-36] use a very simplified model which doesn't take account of drag forces etc; the works in [22, 24-28, 30-32] use feedback linearization whose success depends on exact measurement of parameters; the works in [21, 23, 24, 27-30, 32] did not employ hard maneuvers in simulations, so it is not clear whether their control can result in effective tracking under the constraint of available acceleration limits; most of the control strategies in [22-37] either use rate limiters for dealing with acceleration constraint or do

not address it at all; the work in [23, 29] addressed parametric uncertainties while the other mentioned references do not take account of deviation of model parameters.

Table 1

	Velocity following delay	Settling time	Steady state error	% Overshoot	Acceleration constraint	Remarks
PWL Model	≈ 2.5 s	≈ 12 s	Negligibly small	≈ 4%	considered	Parametric uncertainties addressed Hard maneuvers used.
[21]	Not given	≈ 8 s	Negligibly small	≈ 5%	considered	Parametric uncertainties not addressed Hard maneuvers not used
[22]	<1 s	≈ 17 s	Negligibly small	<1%	Not considered	Parametric uncertainties not addressed Hard maneuvers used
[24]	Not given	≈ 22 s	Negligibly small	≈ 20%	considered	Parametric uncertainties not addressed Hard maneuvers not used
[25]	>8 s	≈ 35 s	Negligibly small	≈ 15%	considered	Parametric uncertainties not addressed Hard maneuvers not used
[28]	<1s	≈ 15 s	Negligibly small	≈ 2.9%	Not considered	Only decel. maneuver addressed Parametric uncertainties not addressed Hard maneuvers not used
[30]	0.4 s	≈ 5 s	Negligibly small	≈ 5%	considered	Variations of only Engine Time Constant considered. Hard maneuvers not used
[31]	Not given	≈ 5 s	Negligibly small	≈ 5%	considered	Variations of Engine Time Constant considered. Hard maneuvers not used
[37]	≈ 3 s	≈ 10 s	Negligibly small	≈ 15%	considered	Robustifying disturbances considered. Parametric uncertainties not addressed Hard maneuvers used
[39]	≈ 5 s	Not given	Negligibly small	≈ 18%	considered	Parametric uncertainties not addressed. Hard maneuvers not used
[40]	≈ 2 s	>40 sec	Negligibly small	≈ 25%	Not given	Parametric uncertainties not addressed Hard maneuvers not used

6. Conclusion

In this paper we have adopted a nonlinear function approximation scheme based on the lattice PWL model. We have outlined its simple and step-by-step modeling procedure, and integrated the modeling scheme with the nonlinear convex VFM. The approximation of the system is achieved by using only three local linear functions covering the entire domain of interest. With this study we concluded that the number of local linear parameters and hence the complexity of modeling and control will depend upon the number of nonlinearities, type of nonlinearities, and the required precision of approximation. Since the number and type of nonlinearity of VFM is favorable, PWL modeling stands as a more promising alternative to the traditional feedback linearization of VFM. Using optimal control by LQR method and gain scheduling logic based on the measurement of velocity, three local linear controllers are designed, which are capable to drive the system to any desired trajectory. The performance analysis is accomplished in simulations, which has shown that the approximation is valid and allows the system to be controlled by linear methods. The effects of parametric uncertainties (being an inescapable element) are also evaluated to determine the robustness of the control system. Our future aim is to apply this modeling technique on a nonlinear system with two or more nonlinearities and address the related control issues.

References

[1] **C. Wen, S. Wang; F. Li, M.J. Khan.** A compact f-f model of high-dimensional piecewise-linear function over degenerate intersection. *IEEE Trans. Circuits and Systems* I, *Vol*.52, 2005, 815-821.

[2] **M. Storace, O.De Feo.** Piecewise Linear approximation of nonlinear dynamical systems. *IEEE Transactions on Circuits and Systems*-1, *Vol*.51, *No.*4, *April* 2004, 830-842.

[3] **L. Vandenberghe, B.L.de Moor, J. Vandewalle.** The generalized linear complementarity problem applied to the complete analysis of resistive piecewise-linear circuits. *IEEE Trans. on Circuits and Systems, Vol*.36, *Issue* 11, *Nov*. 1989,1382-1391.

[4] **C. Kahlert, L.O. Chua.** A generalized canonical piecewise linear representation. *IEEE Trans. Circuits and Systems*, *Vol*.37, *Mar*.1990, 373-383.

[5] **J.N. Lin, X. Hong-Qing, R. Unbehauen.** A generalization of canonical piecewise linear functions. *IEEE Trans. Circuits and Systems*, *Vol*.41, *Apr*. 1994, 345-347.

[6] **E.D. Sontag.** Nonlinear Regulation: The Piecewise Linear Approach. *IEEE Transactions on Automatic Control*. *Vol*.26, *No.*2, *Apr*. 1981, 346-358.

[7] **C. Wen, S. Wang, H. Zhang, M.J. Khan.** A novel compact piecewise-linear representation. *International Journal of Circuit Theory and Applications*, *No.*33, 2005, 87-97.

[8] **G. Feng.** Controller design and analysis of uncertain piecewise linear systems. *IEEE Transactions on Circuits and Systems* I: *Fundamental Theory and Applications*, *Vol*.49, *No.*2, *February* 2002, 28-43.

[9] **S. Wang, K.S. Narendra.** Nonlinear system identification with lattice piecewise-linear functions. *American Control Conference, Vol*.1, 388-393.

[10] **A. Juloski, S. Paoletti, J. Roll.** Recent techniques for the identification of piecewise affine and hybrid systems. *In Current trends in nonlinear systems and control, Birkäuser*, 2006, 77-97.

[11] **J.M. Tarela, M.V. Martínez.** Region configurations for realizability of lattice piecewise-linear models. *Mathematical and Computer Modelling*, *Vol*.30, *No.*11-12, 1999, 17-27.

[12] **F.J. Christophersen, M. Baotic, M. Morari.** Optimal control of piecewise affine systems: A dynamic programming approach. *Lecture Notes in Control and Information Sciences* 322, 2005, 183-198.

[13] **X. Li, S. Wang; Y. Wenjun.** A canonical representation of high-dimensional continuous piecewise-linear functions. *IEEE Trans. Circuits and Systems* I, *Nov*. 2001, 1347-1351.

[14] **S.M. Kang; L.O. Chua.** A global representation of multidimensional piecewise linear functions with linear partitions. *IEEE Trans. Circuits and Systems, Vol*.25, Nov. 1978, 938-940.

[15] **L. Yann, B. Jacques, G. Germain.** Scheduling of local robust laws for nonlinear system control. *Proc. of IEEE Conference on Control Applications, Sep* 2001.

[16] **F. D. Torrisi, A. Bemporad.** HYSDEL – A tool for generating computational hybrid models for analysis and synthesis problems. *IEEE Transactions on Control Systems Technology*, *Vol*.12, *No.*2, *March* 2004.

[17] **L. Ozkan, M.V. Kothare, C. Georgakis.** Model predictive control of nonlinear systems using piecewise linear models. *Elsevier journal of Computers and Chemical Engineering* 24, 2000, 793-799.

[18] **M. S.Padín, J.L. Figueroa.** Use of CPWL approximations in the design of a Numerical Nonlinear Regulator. *IEEE Transactions on Automatic Control*, *Vol*.45, *No.*6, June 2000, 1175-1180.

[19] **J. Billingsley.** On the design of position control systems. *IEE Proceedings- Control Theory and Applications*, *Vol*.138, *No.*4, *July* 1991.

[20] **K.M. Junaid, S. Wang.** Automatic cruise control modeling – a lattice PWL approximation approach. *Intelligent Transportation Systems Conference,* 2006, *ITSC* '06, *IEEE*, 17-20 *Sept*. 2006, 1370-1375.

[21] **S. Sheikholeslam, C. A. Desoer.** Longitudinal control of a platoon of vehicles with no communication of lead vehicle information: a system level study. *IEEE Transactions on Vehicular Technology*, *Vol*.42, *Issue* 4, *Nov*. 1993, 546-554.

[22] **P.A. Ioannou, C.C. Chien.** Autonomous intelligent cruise control. *IEEE Transactions on Vehicular Technology, Vol*.42, *Issue* 4, *Nov*. 1993, 657-672.

[23] **D. Swaroop, J.K. Hedrick, S.B. Choi.** Direct Adaptive Longitudinal Control of Vehicle Platoons. *IEEE Transactions on Vehicular Technology*, *Vol*.50, *No.*1, *January* 2001, 150-161.

[24] **X. Huppe, J. de Lafontaine, M. Beauregard, F. Michaud.** Guidance and control of a platoon of vehicles adapted to changing environment conditions. 2003 *IEEE International Conference on Systems, Man and Cybernetics, Vol*.4, 5-8, *Oct*. 2003, 3091-3096.

[25] **P. Ioannou, Z. Xu, S. Eckert, D. Clemons, T. Sieja.** Intelligent cruise control: theory and experiment. 32*nd IEEE Conference on Decision and Control, Vol*.2, 15-17 *Dec*. 1993, 1885-1890.

[26] **D.N. Godbole, J. Lygeros.** Longitudinal control of the lead car of a platoon. *IEEE Transactions on Vehicular Technology, Vol*.43, *No.*1, 1994, 1125-1135.

[27] **A. Stotsky, C. C. Chien, P. Ioannou.** Robust Platoon-Stable Controller Design for Autonomous Intelligent Vehicles. *Proceedings of the* 33*rd conference on Decision and control, December* 1994, 2431-2435.

[28] **S. Huang, W. Ren.** Vehicle longitudinal control using throttles and brakes. *Elsevier Journal of Robotics and Autonomous Systems*, *No.*26, 1999, 241-253.

[29] **A.K. Sanyal, M. Chellappa, J.L. Valk, J. Ahmed, J. Shen, D.S. Bernstein.** Globally convergent adaptive tracking of spacecraft angular velocity with inertia identification and adaptive linearization. *Proceedings.* 42*nd IEEE Conference on Decision and Control Vol*.3, Dec. 2003, 2704-2709.

[30] **S.S. Stanković, M.J. Stanojević, D.D. Siljak.** Decentralized Overlapping Control of a Platoon of Vehicles. *IEEE Trans. on Control Systems Technology, Vol*.8, *Issue* 5, Sept. 2000, 816-832 .

[31] **T.S. No, K.-T. Chong, D.-H. Roh.** A Lyapunov Function Approach to Longitudinal Control of Vehicles in a Platoon. *IEEE Transactions on Vehicular Technology, Vol*.50, *No.*1, 2001, 116-124,,.

[32] **K. Santhanakrishnan, R. Rajamani.** On spacing policies for highway vehicle automation**.** *IEEE Transactions on Intelligent Transportation Systems, Vol*.4, *Issue* 4, *Dec*. 2003, 198-204.

[33] **C.Y. Liang, H. Peng.** Optimal Adaptive Cruise Control with Guaranteed String Stability. *Vehicle System Dynamics,* 31, 1999, 313-330.

[34] **R. Rajamani, C. Zhu.** Semi-Autonomous Adaptive Cruise Control Systems. *IEEE Transactions on Vehicular Technology*, *Vol*.51, *No.*5, *September* 2002, 1186-1192.

[35] **J. Wang, R. Rajamani.** Should adaptive cruise-control systems be designed to maintain a constant time gap between vehicles? *IEEE Transactions on Vehicular Technology*, *Vol*.53, *No.*5, September 2004, 1573-1585.

[36] **S. Huang, W. Ren.** Longitudinal control with time delay in platooning. *IEE Proc.-Control Theory Appl.*, *Vol*.1.15, *No.*2, *March* 1998, 211-217.

[37] **S. Seshagiri, H. Khalil.** Longitudinal adaptive control of a platoon of vehicles. *Proceedings of the Amer. Contr. Conference, June* 1999.

[38] **M. Babaali, M. Egerstedt.** Observability of switched linear systems. *Hybrid Systems: Computation and Control (R. Alur and G. Pappas, eds.).Springer*, 2004, 48-63.

[39] **L. Bin, W. Rongben, C. Jiangwei.** A New Optimal Controller for Intelligent Vehicle Headway Distance. *IEEE Intelligent Vehicle Symposium*, 2002.

[40] **C. Hatipoglu, U. Ozguner, M. Sommerville.** Longitudinal headway control of autonomous vehicles. *IEEE Intl Conf. on Control Applications,* 1996,721-726.

Received December 2009.